Learning Science Through Research
Published by the Keck Geology Consortium
Short Contributions
Keck Geology Consortium
Volume 37
May 2025
doi: 10.18277/AKRSG.2025.37.02

CONSTRAINING HIGH-DISPLACEMENT FAULT DAMAGE EVOLUTION WITHIN THE SEVIER FAULT SYSTEM, SOUTHERN UTAH

SYDNEY COSTA, West Chester University
Project Advisor: Benjamin Surpless

INTRODUCTION

The geometry and structure of damage zones are primarily influenced by their position relative to a fault, the way slip occurs at the fault tip, and the stage of fault evolution. While lithology, rock strength, and regional stress conditions also shape damage zones, understanding their development requires analyzing the three-dimensional fault geometry and how movement occurs at fault tips (e.g., Kim et al., 2004). Modeling these systems allows us to study how these faults propagate and evolve. It also provides insight into fluid flow, guides seismic risk assessment, and helps us understand fault growth and the interaction with nearby faults.

A key topic of debate in fault mechanics is how damage zones evolve with increasing displacement. Some researchers suggest that the width and displacement of the damage zone are proportional and increase at a constant rate. Others argue that a rapid growth period occurs before displacement and is followed by a slower growth rate (e.g., Savage and Brodsky, 2011; Mayolle et al., 2021; 2023). In addition to damage zone mechanics, research has demonstrated that lithological characteristics play a key role in fault evolution (e.g., Fossen, 2016). For example, brittle rocks like sandstone break into numerous minor fractures, creating pathways for fluid movement, while ductile rocks such as shale deform more plastically, which limits permeability and alters how stress is distributed (e.g., Fossen, 2016).

The Sevier Fault, located in southern Utah, is an ideal study area for investigating this topic. The fault has a range of displacements from 2.5 to 800 meters. Mapping by Taylor et al. (2024) reveals a well-constrained network of faults, which allows for a more comprehensive study of damage zone development over time. Conceptual models have provided a foundation for understanding damage zone growth within the Sevier fault (Taylor et al., 2024). However, significant debate remains regarding how displacement alone influences fault damage characteristics. Thus, the Sevier Fault allows us to evaluate hypotheses of damage zone development by analyzing a natural system with a well-documented structural history (Taylor et al., 2024). This study will explore the development of damage zones in large-displacement normal faults to provide insight into the broader mechanisms that shape fault zones and associated geological processes.

GEOLOGIC BACKGROUND

The Sevier Fault is a west-dipping normal fault located in southern Utah between the Basin and Range Province and the Colorado Plateau. It is part of the more extensive Toroweap-Sevier fault system and extends over 300 kilometers (Surpless, this volume). Near the Mount Carmel segment, the Sevier Fault shows a significant vertical displacement of approximately 800 meters (Taylor et al., 2024). While it is currently an active normal fault, the region's geologic history is rooted in earlier compressional deformation from the Sevier and Laramide orogenies. Between ~170 and 40 million years ago, the Sevier thrust system, documented on the surface to the west but possibly also active in buried faults beneath the study area, formed during this mountain-building event, driven by the subduction of the Farallon plate (e.g., Willis, 2000). Thus, the modern Sevier normal fault may have reactivated a deeper basement-level reverse fault as tectonics shifted from compression to extension in Miocene time (e.g., Taylor et al., 2024).

Field study reveals contrasting lithologies on either side of the fault, strongly influencing deformation style, damage zone development, and landscape development. The eastern footwall consists primarily of the Lower Jurassic Navajo Sandstone, a resistant, cross-bedded aeolian sandstone characterized by its reddish-orange color and cliffs due to its erosion resistance (Utah Geological Survey, n.d.). Research by Surpless and McKeighan (2022) demonstrated that fracture branching within this unit is crucial for developing complex fracture networks, which enhance permeability and accommodate strain within the damage zone. In contrast, the western hanging wall is dominated by the Cretaceous Tropic Shale, a fine-grained marine shale whose weaker lithology results in greater deformation within the fault zone (Utah Geological Survey, n.d.).

CONCEPTUAL BACKGROUND

Normal fault evolution is a complex process, and in southern Utah, the Sevier Fault provides a well-documented zone with varying displacements. Faults typically initiate as isolated segments growing laterally and vertically until interaction (e.g., Fossen, 2016). As their tips approach, faults may underlap, with their stress fields interacting before a physical connection forms (e.g., Crider and Pollard, 1998; Peacock, 2002). Over time, these interactions can lead to linkage, progressing from soft-linked systems to hard-linked continuous fault surfaces. Field mapping within the Mount Carmel segment suggests such a progression has occurred. Fault tips in this area appear to have overlapped and ultimately connected through breakthrough faults, forming hard linkage structures (Taylor et al., 2024).

As faults propagate and link, displacement accumulates, generally producing a bell-shaped displacement profile characterized by maximum displacement at the fault center and tapering towards the tips (Fossen, 2016). However, displacement patterns can become more complex in linked fault systems due to mechanical interaction between segments (Fossen, 2016). Closely associated with fault growth and displacement is the development of damage zones, regions of fractured and deformed rock surrounding the fault core. As faults evolve, they typically produce both a fault core and damage zones. The inner damage zone is marked by intense, closely spaced fracturing, while the outer damage zone exhibits lower fracture density and accommodates less strain (e.g., Berg and Skar, 2005). An unresolved question revolves around how damage zones evolve with increasing fault displacement. This highlights the need for studies that evaluate natural fault systems with well-documented displacement histories to help constrain and refine models of fault growth and damage zone evolution.

METHODS

Field

In the field, we documented the position and orientation of fractures along the Mt. Carmel segment, where the fault has accumulated ~800 m displacement. At each outcrop, we documented fractures 3 meters long or greater. For each fracture, the dip, dip direction, spatial position, and spacing relative to the previous fracture were recorded. We utilized a handheld GPS for accurate geolocation. We compiled detailed field documentation, including photographs and structural data and description. In areas where direct observation was not practical, a DJI Mavic 3 Unmanned Aerial Vehicle (UAV) was utilized to collect high resolution imagery and video of selected fault damage zone exposures. Three-dimensional models were created using Structure-from-Motion (SfM) techniques with Agisoft Metashape software (Johnson et al., 2014). This program takes overlapping images and utilizes an algorithm to match common points between images. Models of the fracture network were built, refined, and textured using the image data to ensure a realistic and detailed representation (Fig. 1).

The Mt. Carmel segment of the Sevier Fault has well-exposed outcrops of the hanging wall damage zone, including where the fault has accommodated ~800 m displacement (see 3 in Fig. 3 from Surpless, this volume). I aimed to document the structure and

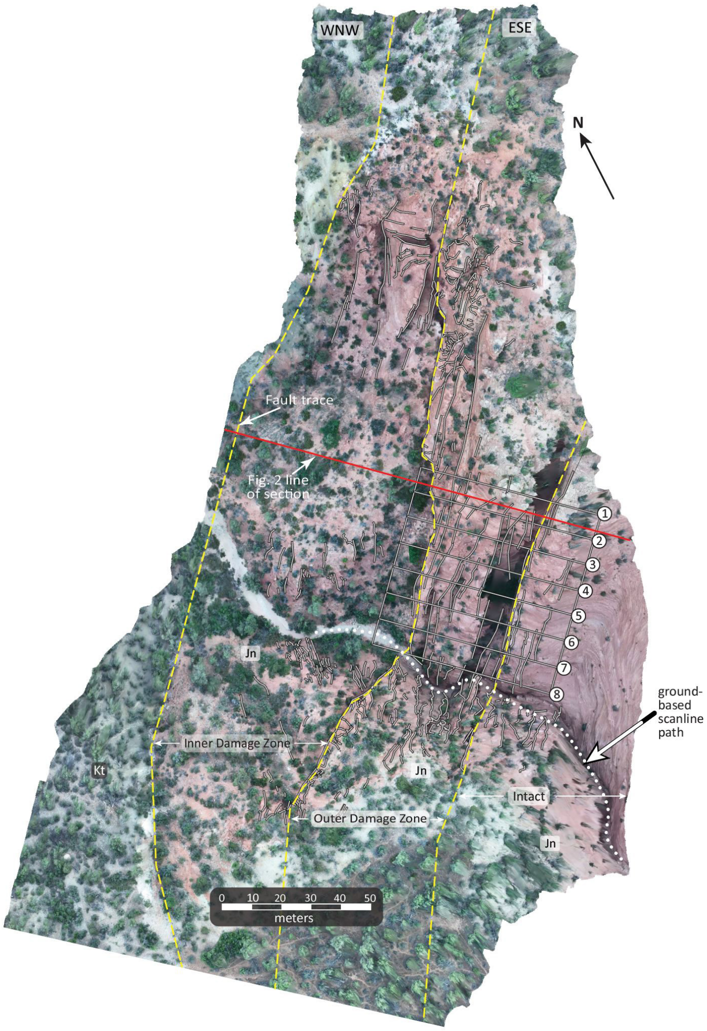

Figure 1. Orthomosaic computer model of the main study area. The dashed yellow lines represent (from left to right) the Mt. Carmel segment of the fault, the inner damage zone, the outer damage zone, and the intact rock with minimal damage. The white dotted line represents the path taken to measure the ground-based scanline. The fault strikes north-northeast.

fracture characteristics within the footwall damage zone and examine how width and internal structure of the damage zone and fracture intensity scale with displacement relative to a location in the same lithology with much lower accumulated displacement (see 1 in Fig. 3 from Surpless, this volume). Both sites (high- and low-displacement localities), expose the Jurassic Navajo Sandstone in the footwall, allowing direct comparison of damage zone characteristics. In addition, at the high-displacement locality, accumulated displacement now juxtaposes the Cretaceous Tropic Shale in the hanging wall against the Jurassic Navajo Sandstone in the footwall, permitting us to compare damage zone characteristics across lithologies with contrasting strengths. Finally, to examine internal fault architecture, a trench was excavated across the fault core at an outcrop, allowing direct observation of fault rock composition and geometry.

Scanline Analysis

Fracture spacing and intensity were quantified using two approaches: a ground-based scanline survey and scanlines from the 3D SfM model. These data were used to calculate fracture intensity (F.I.) and the modified coefficient (C_V') (Hooker et al., 2023) as follows:

$$\text{F.I.} = n/L \qquad (1)$$

$$C_V' = \sigma/M \qquad (2)$$

Where n is the number of fractures, and L the total length of the scanline. In (2), σ and M reflect the standard deviation and median of our spacing measurements, respectively. Fracture intensity measures the frequency of fractures along a scanline. High fracture intensity values may indicate zones of concentrated strain deformation. Low fracture intensity values suggest an area of lower strain, where fractures are fewer and more widely spaced. The modified coefficient of variation quantifies the variability in fracture spacing. A low C_V' indicates more regular fracture spacing, while a high C_V' indicates clustering of fractures (Hooker et al., 2023).

RESULTS AND DISCUSSION

Based on field observations and the construction of a 3D SfM model (Fig. 1), we classified three main structural domains within footwall damage zones exposed along the Mt. Carmel fault segment: a fault core, an inner damage zone, and an outer damage zone (Fig. 2). The fault core is narrow (~80 cm across) and highly strained without any intact rock other than minor inclusions in the pulverized matrix (Fig. 3), and the inner damage zone has a high fracture intensity. In contrast, the outer damage zone is less intensely fractured and grades into intact rock. The total width of the footwall damage zone varied from 100-120m wide at this locality (Fig. 1).

A ground-based scanline with position measured perpendicular to the fault plane at location E across

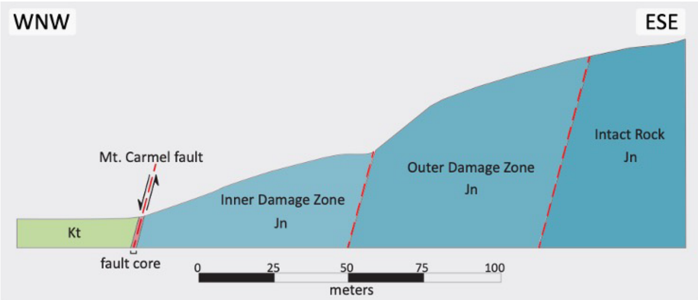

Figure 2. Topographic profile across the main study area shown in Fig. 1. Note how topographic expression reflects damage zone structure.

the entire footwall damage zone (Fig. 1) revealed a fracture intensity of 0.36 fractures per meter, with a C_V' value of 1.09. A stereonet plot displays the orientations of fractures from the ground-based scanline, illustrating very steep, NNE-striking fracture sets consistent with shear fracturing in a stress field with a tensional minimum stress axis (Fig. 4).

The 3D model-derived scanlines (8 total) focused on the outer damage zone showed the same fracture intensity (0.36 fractures per meter) with a higher C_V' value of 3.03, suggesting a more clustered fracture population. We suggest that the easier documentation of fractures on a ground-based scanline relative to an SfM model means that we will identify more fractures, on average, resulting in a higher fracture intensity at the same location. This would explain why the ground-based scanline displays the same fracture intensity despite involving a significant thickness of relatively intact rock outside the outer damage zone (Fig. 1).

The difference in C_V' values reveals significant fracture clustering across the outer damage zone relative to the broader footwall damage zone and intact rock measured by the ground-based scanline. These high C_V' values indicate a disorganized, less predictable fracture network, which is common within fault damage zones (e.g., Peacock et al., 2016; Surpless and McKeighan, 2022) and contrasts with the more regularly spaced fractures typically documented in rock affected by less focused regional tectonic stresses (e.g., Peacock et al., 2016).

The relatively small differences between the width of the footwall damage zones documented here (~100-120 m) and those documented by Ryter (this

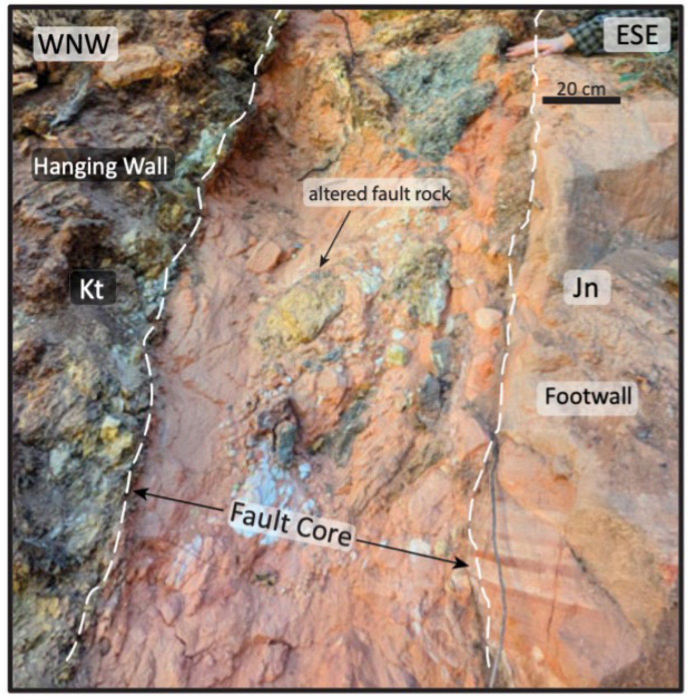

Figure 3. Cross-sectional view of the Mt. Carmel segment fault core.

volume) (~40 – 50 m) for the same lithology and fault network, in spite of a very large difference in displacement (~800 m in this study versus less than 2.5 m in the study by Ryter, this volume), suggests that damage zone dimensions do not scale linearly with displacement, consistent with Mayolle et al. (2023). Similarly, despite the same differences in displacement, fracture intensity remains consistent (this study and Ryter, this volume). This similarity suggests that fracture intensity within the damage zone does not scale linearly with displacement. This pattern aligns with the fault zone evolution model proposed by Torabi et al. (2019; 2020), who observed that deformation increasingly localizes within the fault core as displacement accumulates. As the fault matures, a larger proportion of strain is accommodated within the core, reducing damage across the rest of the damage zone (Torabi et al., 2019).

Thus, damage zone growth and the related intensity of fracturing may be decoupled from displacement in more mature fault systems (Mayolle et al., 2021). We also note that once displacement reached a value so that the Cretaceous Tropic Shale in the hanging wall contacted the Jurassic Navajo Sandstone in the footwall, it is likely that the weaker Tropic Shale accommodated most new strain, fundamentally inhibiting the generation of new fractures in the

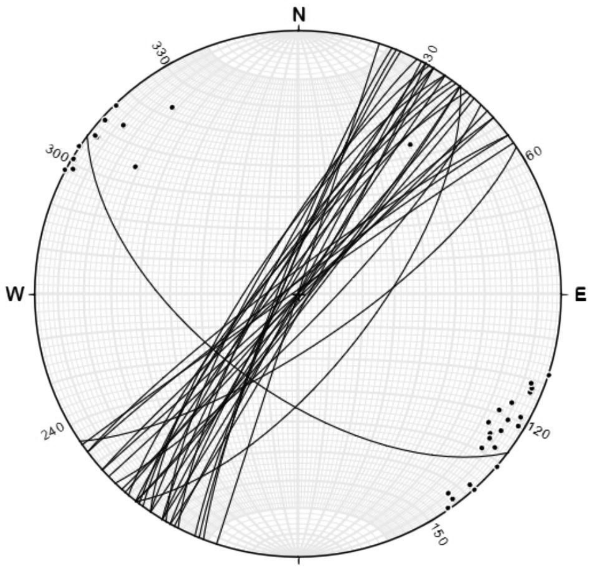

Figure 4. Lower-hemisphere equal-area stereonet displaying fault plane orientations measured along the ground-based scanline shown in Fig. 1.

Navajo Sandstone.

The difference in how lithology accommodates extension is best displayed adjacent to the fault core (Fig. 3), where the strong Navajo Sandstone shows only minor deformation in the footwall, with preserved bedding and limited to no brecciation. In contrast, the Tropic Shale in the hanging wall is heavily brecciated and contains numerous inclusions in a shale-rich matrix, reflecting the unit's mechanical weakness to the point that ductile deformation plays a significant role, with fracturing less likely. This is consistent with findings by Shipton and Cowie (2003), who observed that highly porous and competent sandstones, such as the Navajo, tend to develop dense fracture networks that accommodate strain across broader zones relative to weaker lithologies like shales.

Based on our data, the lack of correlation between displacement, damage zone width, and fracture intensity in the Mt. Carmel segment can be explained by: 1) the increase in the percentage of strain accommodated within the fault core, which inhibits an increase in fault damage zone width; and 2) the strong contrast between lithologies in contact across the fault plane once enough displacement had accumulated – when the shale in the hanging wall came into contact with the sandstone in the footwall, any damage zone widening or increase in fracture intensity within the footwall would likely have ceased.

CONCLUSION

The study of the Mt. Carmel segment of the Sevier Fault highlights the crucial interplay between lithology and fault zone evolution in a high-displacement setting. With displacements reaching up to ~800 meters, this segment provides an ideal natural laboratory for evaluating how large-displacement faults accommodate strain. Our observations, supported by insights from Torabi et al. (2019) and Shipton and Cowie (2003), demonstrate that lithologic contrasts and the increase in accommodation of strain by the fault core strongly influence fault damage zone architecture and evolution.

Despite significant variation in displacement along the fault, fracture intensity and damage zone width remain relatively constant, indicating that displacement does not scale linearly with damage zone width or fracture intensity. Instead, as the fault matures, deformation becomes increasingly localized within the fault core, and lithologic contrasts across the fault plane also play an important role. These findings have implications for structural analysis and fault modeling. These results also inform structural applications to natural resource exploration and geohazard assessment.

ACKNOWLEDGEMENTS

This material is based upon work supported by the Keck Geology Consortium and the National Science Foundation under Grant No. 2050697. Funding for this project was provided by a 2024-2025 Keck Geology Consortium Advanced Research Project Grant as part of an NSF-REU Award to the Keck Geology Consortium (EAR 1659322; PIs Wirth, K., and Davidson, C.). Funding was also provided by NSF Award 2042114 to PI Surpless.

REFERENCES

Cailleau, B., Walter, T.R., Janle, P., and Hauber, E., 2003, Modeling volcanic deformation in a regional stress field: Implications for the formation of graben structures on Alba Patera, Mars: Journal of Geophysical Research: Planets,

v. 108, doi: 10.1029/2003je002135.

Crider, J.G. and Pollard, D.D., 1998, Fault linkage: three-dimensional mechanical interaction between echelon normal faults: Journal of Geophysical Research, v. 103, p. 24,373-24,391.

Grant, J.V., and Kattenhorn, S.A., 2004, Evolution of vertical faults at an extensional plate boundary, southwest Iceland: Journal of Structural Geology, v. 26, p. 537-557.

Hauber, E., Grott, M., and Kronberg, P., 2010, Martian rifts: Structural geology and geophysics: Earth and Planetary Science Letters, v. 294, p. 393-410, https://doi.org/10.1016/j.epsl.2009.11.005.

Ivanov, M. A., & Head, J. W. (2006). Alba Patera, Mars: Topography, structure, and evolution of a unique late Hesperian–early Amazonian shield volcano. Journal of Geophysical Research, 111(E9). https://doi.org/10.1029/2005je002469

Koehn, D., A. Steiner, and K. Aanyu (2019), Modelling of extension and dyking-induced collapse faults and fissures in rifts, Journal of Structural Geology, 118, 21–31, doi: 10.1016/j.jsg.2018.09.017.

McGovern, P.J., Solomon, S.C., Head, J.W., Smith, D.E., Zuber, M.T., and Neumann, G.A., 2001, Extension and uplift at Alba Patera, Mars: Insights from mola observations and loading models: Journal of Geophysical Research: Planets, v. 106, p. 23769–23809, doi: 10.1029/2000je001314.

McMillin, A.M., 2013, Assessment of Linkage Likelihood in Segmented Normal Fault Systems in the Tharsis Region, Mars, [MS Thesis]: University of Alaska at Anchorage

Öhman, T., and McGovern, P. J., 2014, Circumferential graben and the structural evolution of Alba Mons, Mars. Icarus, 233, 114–125. https://-doi.org/10.1016/j.icarus.2014.01.043

Peacock, D., 2002, Propagation, interaction and linkage in normal fault systems: Earth-Science Reviews, vol. 58, nos. 1–2, p. 121–142.

Polit, A.T., Schultz, R.A., and Soliva, R., 2009, Geometry, displacement–length scaling, and extensional strain of normal faults on Mars with inferences on mechanical stratigraphy of the Martian crust: Journal of Structural Geology, v. 31, p. 662–673, doi: 10.1016/j.jsg.2009.03.016.

Rivalta, E., B. Taisne, A. P. Bunger, and R. F. Katz, 2015, A review of mechanical models of dike propagation: Schools of thought, results and future directions, Tectonophysics, v. 638, p. 1–42, doi: 10.1016/j.tecto.2014.10.003.

Rubin, A. M., and D. D. Pollard (1988), Dike-induced faulting in rift zones of iceland and afar, Geology, 16(5), 413, doi: 10.1130/0091-7613(1988)016<0413:difirz>2.3.co;2.

Scott, D.H., and Tanaka, K.L., 1980, in Lunar and Planetary Science Conference Proceedings, Houston, Pergamon Press, v. 3, p. 2403–2421.

Scott, E., and L. Wilson (2003), Did the Alba Patera and Syria Planum regions of Mars lose their lithospheric roots in convective overturn events? J. Geophys. Res., 108, 5035, doi:10.1029/2002JE001492, E5.

Tanaka, K.L., Davis, P.A., and Golombek, M.P., 1989, Development of grabens, tension cracks, and pits southeast of Albe Patera, Mars, In T.R. Watters and M.P. Golombek, Eds., MEVIV Workshop on Tectonic Features on Mars: LPI Technical Report 89-06, Lunar and Planetary Institute, Houston.

Tanaka, K.L., 1990, Tectonic History of the Alba Patera-Ceraunius Fossae Region of Mars, in Lunar and Planetary Science Conference Proceedings, Houston, TX, Branch of Astrogeology, US Geological Survey, p. 515–523.

Tanaka, K.L., 2014, The new geologic map of mars: Guiding research and education: Eos, Transactions American Geophysical Union, v. 95, p. 341–342, doi: 10.1002/2014eo380001.

Taylor, W., Surpless, B., Schiefelbein Kerscher, I., 2024, Complex Segment Linkage Along the Sevier Normal Fault, Southwestern Utah: Lithosphere, Special v. 15, doi: /10.2113/2024/lithosphere_2023_332.

Wiedeking, S., Lentz, A., Pasckert, J.H., Raack, J., Schmedemann, N., and Hiesinger, H., 2023, Rheological properties and ages of lava flows on Alba Mons, Mars: Icarus, v. 389, p. 115267, doi: 10.1016/j.icarus.2022.115267